

Local Convertibility in 1D Magnetic Systems

Bernard Faulend

Department of Physics, Faculty of Science, University of Zagreb, Bijenička cesta 32, 10000 Zagreb, Croatia

Advisors: dr. sc. Fabio Franchini, dr. sc. Salvatore Marco Giampaolo
Ruder Bošković Institute, Bijenička cesta 54, 10000 Zagreb, Croatia

(Dated: January 21, 2025)

Local convertibility is a powerful tool to investigate entanglement properties of many-body systems, since it is a local probe of long-range entanglement. Here, we investigate local convertibility of spin-1/2 XY chain and the effects of frustration on local convertibility. We show that local convertibility is generally not a property of a quantum phase, and observe qualitative differences between frustrated and unfrustrated XY chains, even in thermodynamic limit. Results are also relevant for other frustrated spin models that share the approximate generalized W state structure of their ground states.

I. INTRODUCTION

Entanglement is one of the most distinctive phenomena in quantum mechanics. It is conceptually central to quantum physics, but it is very distant from what we observe in everyday life and it has no counterpart in classical physics. Presence of entanglement makes our description of the physical world inherently non-local since a state describing a set of spatially separated particles cannot be decomposed to states of individual particles. With the rapid experimental advances in recent years, entanglement is no longer just a theoretical curiosity, but a keystone of novel technologies such as quantum computing.

A deep understanding of entanglement properties is necessary not only for quantum technologies, but also to gain insight in behavior of interacting quantum many-body systems, that can lead to exotic new phenomena in condensed matter and atomic physics [1–3]. In fact, studying entanglement allows us to make connections between many-body quantum physics and quantum computing since entanglement present in many-body quantum systems can be viewed as a resource for quantum computation, and many-body systems such as atoms in optical lattices can be used as quantum simulators [4]. Furthermore, entanglement properties are crucial to understand if a quantum system can be efficiently classically simulated or not, and it is only in the latter case that quantum advantage can be obtained when a system is used as a quantum simulator. However, it is generally a difficult problem to determine if a quantum system is classically simulatable and there are some types of highly entangled states that can be efficiently classically simulated [5]. Thus, for a state of a many-body system, distribution and possibility of effectively using entanglement can be even more important than the sheer amount of it [6, 7].

An elegant way to investigate some properties of entanglement in many-body systems is by studying local convertibility. Given a many-body quantum system AB that is partitioned to subsystems A and B, a quantum state

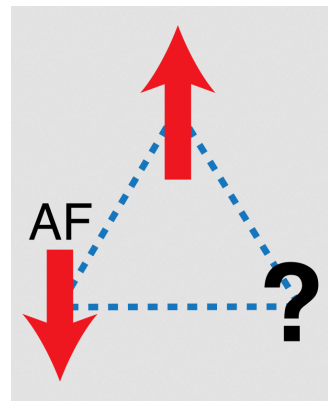


FIG. 1: Antiferromagnetic interactions, periodic boundary conditions and odd number of spins lead to frustration.

$|\psi_1\rangle$ of the system AB is locally convertible to state $|\psi_2\rangle$ if $|\psi_1\rangle$ can be transformed to $|\psi_2\rangle$ through Local Operations and Classical Communication (LOCC) restricted to subsystems A and B [8]. It can be shown that $|\psi_1\rangle$ is locally convertible to $|\psi_2\rangle$ if and only if $|\psi_2\rangle$ is less entangled than $|\psi_1\rangle$. Correspondingly, absence of local convertibility implies presence of long-range coherence between A and B that cannot be captured classically.

Here, we study local convertibility of ground states in one-dimensional spin-1/2 XY chain. More specifically, we choose a path in space of parameters that determine the Hamiltonian of XY model, and determine if ground states of the Hamiltonian are locally convertible when the parameters are changed along the path. Although seemingly artificial, 1D spin models are relevant both because they can capture the essential physics of more complex models and because they can be directly experimentally implemented, e. g. using cold atom quantum simulators [9]. We also investigate the effects of topological frustration on local convertibility. Topological frustration is present in a system with frustrated boundary conditions

(FBC), i. e. periodic boundary conditions with antiferromagnetic interactions and odd number of spins. FBCs prevent the simultaneous minimization of all interaction terms in the Hamiltonian as illustrated on Fig. 1. This leads to higher degeneracy of ground state and various interesting effects such as the presence of a quantum phase transition induced by boundary conditions [10]. We show that presence of topological frustration has significant effects on local convertibility, especially in the part of frustrated XY chain parameter space known as the chiral region [11].

The seminar is structured as follows: in section 2 we discuss general properties and phase diagram of the XY model, and we outline the procedure for investigating local convertibility by evaluating Renyi entropies and their derivatives. In section 3 we present and discuss the results we obtained for unfrustrated XY chain, first we briefly expose the results for Ising chain and edge state recombination mechanism that can destroy local convertibility, and then we discuss the effects of so-called factorization line which are in some cases reminiscent of a phase transition. In section 4, we discuss the results obtained for frustrated XY chain and relate our findings to a more general class of frustrated spin chains by investigating local convertibility of generalized W states. After that, we give our concluding remarks in section 5.

II. MODEL AND METHODS

XY model is a paradigmatic spin chain that is exactly solvable in one dimension. It was first proposed in 1961 by Lieb, Schultz and Mattis [13], and can be described with the Hamiltonian

$$H = J \sum_{j=1}^N \left(\frac{1+\gamma}{2} \sigma_j^x \sigma_{j+1}^x + \frac{1-\gamma}{2} \sigma_j^y \sigma_{j+1}^y - h \sigma_j^z \right), \quad (1)$$

where σ_j^α are Pauli- α matrices ($\alpha = x, y, z$) at j -th site of the chain, γ is the anisotropy parameter and h is transverse field strength. Symmetries allow us to consider only the region in parameter space with $h \geq 0$, $\gamma \geq 0$ because $\pi/2$ rotation around z -axis corresponds to $\gamma \rightarrow -\gamma$ transformation, and reflection about xy -plane corresponds to $h \rightarrow -h$ transformation. FBCs are present in a system with antiferromagnetic interactions ($J > 0$, without loss of generality we can choose $J = 1$), odd chain length N , and periodic boundary conditions $\sigma_j^\alpha = \sigma_{j+N}^\alpha$. The exact solution of transverse-field XY chain can be obtained by mapping the Hamiltonian (1) to a free fermionic form [13], and it is briefly described in the Appendix for a frustrated chain.

Phase diagram of the XY chain at zero temperature is shown on Fig. 2. There are two quantum phase transitions (i. e. phase transitions with the system in the ground state at zero temperature due to changing parameters of the Hamiltonian): (anti)ferromagnetic to paramagnetic transition at $h = 1$ and interval $0 \leq h \leq 1$ of

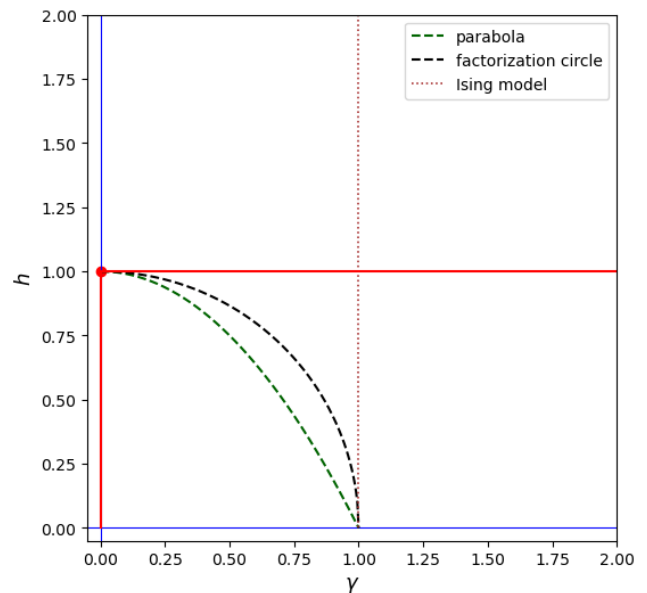


FIG. 2: Phase diagram of XY chain. $h > 1$ region is paramagnetic phase, and $h < 1$ region is (anti)ferromagnetic phase, depending on sign of J . For $h < 1$ we can further distinguish oscillatory region $h^2 + \gamma^2 < 1$ for unfrustrated XY model [12] (inside the factorization circle) and chiral region $h < 1 - \gamma^2$ for frustrated XY model (inside the $h = 1 - \gamma^2$ parabola) [11]. For $\gamma = 1$, XY model reduces to Ising model.

$\gamma = 0$ line, also called XX model. We also note that the famous Ising model is a special case of XY model with $\gamma = 1$.

In unfrustrated XY model, on the $h^2 + \gamma^2 = 1$ circle, ground state is exactly twofold degenerate and there is a factorized (i. e. not entangled) state in the ground state subspace. Above the factorization line ($h^2 + \gamma^2 > 1$), ground state always has even parity, where parity operator is defined with $\Pi_z = \prod_{i=1}^N \sigma_i^z$. On the other hand, parity of the ground state in $h^2 + \gamma^2 < 1$ region has a series of crossovers between even and odd, with the crossovers becoming more and more dense with increasing N . On the factorization line, ground states in even and odd sectors have the same energy leading to the aforementioned degeneracy. Factorization line does not exist in the frustrated model, but again there is a region of parameter space with even ground state parity and region with crossovers in ground state parity. Border of these two regions is $h = 1 - \gamma^2$ parabola. Region with crossovers is $h < 1 - \gamma^2$, which is also called the chiral region since the ground state is exactly twofold degenerate, and ground state subspace is spanned by two states with opposite momenta (see the Appendix).

In order to study local convertibility of XY chain ground states, we divide the chain in two subchains with L and $N - L$ spins and investigate entanglement between the subchains when the whole chain is in XY model

ground state $|\psi\rangle$. Technically, we quantify the amount of entanglement between the subchains through Renyi entropies, which are defined with

$$S_\alpha = \frac{1}{1-\alpha} \log \left(\text{Tr}(\rho_A^\alpha) \right) \quad (2)$$

Here, reduced density matrix (RDM) is defined with $\rho_A = \text{Tr}_B |\psi\rangle \langle \psi|$, and $\alpha \in [0, \infty]$ is a parameter that tunes the relative importance of RDM eigenvalues. For example, $S_0 = \log R$ depends only on number of non-zero eigenvalues (where R is the Schmidt rank of a state), $S_1 = -\text{Tr}(\rho_A \log \rho_A)$ is the von Neumann entropy, and $S_\infty = -\log(\lambda_{max})$ depends only on the largest RDM eigenvalue. Schmidt decomposition guarantees that Renyi entropies for subsystems A and B are the same. A standard result in quantum information theory [14, 15] allows us to reformulate the statement " $|\psi_1\rangle$ is locally convertible to $|\psi_2\rangle$ " if and only if $|\psi_2\rangle$ is less entangled than $|\psi_1\rangle$ " in a more precise way: $|\psi_1\rangle$ is locally convertible to $|\psi_2\rangle$ if and only if $S_\alpha(\rho_1) \geq S_\alpha(\rho_2)$ for all $\alpha \in [0, \infty]$, where $\rho_{1,2} = \text{Tr}_B |\psi_{1,2}\rangle \langle \psi_{1,2}|$.

Typically, we would expect entanglement between the subsystems to increase when parameters in the Hamiltonian are moved closer to a phase transition. Specifically, Schmidt rank R of a state increases as correlation length increases, because more degrees of freedom become entangled. This leads to increasing S_0 , and generally small- α Renyi entropies. However, if there is long-range entanglement (LRE) that cannot be captured with local correlations, and if LRE decreases with correlation length, it is possible that Renyi entropies with higher α decrease when we approach a phase transition [16]. Thus, absence of local convertibility in all directions indicates that there is LRE in the system's ground state. Furthermore, study of local convertibility allows us to detect LRE by only considering small subsystems. An example of a physical mechanism that causes decrease of LRE as phase transition is approached is edge state recombination. Edge states are states that are localized around the boundaries of the system, and they usually exist as a consequence of topological order [17]. When a system is divided into subsystems, new edge states appear at the boundaries between the subsystems, and if the size of a subsystem becomes comparable to correlation length in vicinity of a phase transition, edge states can undergo recombination that reduces LRE between them.

The easiest way to evaluate Renyi entropies in our case is through spin correlation functions, as correlation matrix has only $O(L^2)$ elements for subsystem size L . RDM has $O(2^L)$ elements which makes direct calculation from RDM eigenvalues numerically intractable except for small L . Correlation functions can be conveniently expressed using Majorana fermions A_i, B_i , which are defined in the Appendix. When we make a partition of the system with N spins to 2 blocks of L and $N-L$ consecutive spins, Renyi entropies of RDMs of the subsystems

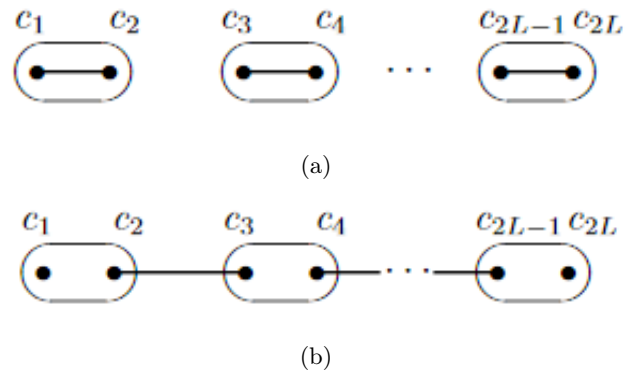


FIG. 3: Pairing of Majorana fermions: (a) on-site interactions stronger than inter-site interactions, (b) inter-site interactions stronger than on-site interactions, leading to existence of edge states. Figure taken from Ref. [19].

are given with [16, 18]

$$S_\alpha = \frac{1}{1-\alpha} \sum_{j=1}^L \log \left(\left(\frac{1+\nu_j}{2} \right)^\alpha + \left(\frac{1-\nu_j}{2} \right)^\alpha \right) \quad (3)$$

Here ν_j are positive eigenvalues of $2L \times 2L$ hermitian correlation matrix defined with $C_{2i,2j+1} = \langle A_i B_j \rangle$, $C_{2i+1,2j} = \langle B_i A_j \rangle$, $C_{2i,2j} = \langle A_i A_j \rangle - \delta_{i,j}$, and $C_{2i+1,2j+1} = \langle B_i B_j \rangle - \delta_{i,j}$. RDM eigenvalues can be obtained as [16]

$$\{\lambda_l\} = \prod_{j=1}^L \left(\frac{1 \pm \nu_j}{2} \right) \quad (4)$$

with all possible combinations of plus/minus signs. If the trajectory in $\gamma - h$ plane is parametrized by t , from Eq. (3) we obtain the expression for the derivative of S_α :

$$\frac{dS_\alpha}{dt} = \frac{\alpha}{1-\alpha} \sum_{j=1}^L \frac{(1+\nu_j(t))^{\alpha-1} - (1-\nu_j(t))^{\alpha-1}}{(1+\nu_j(t))^\alpha + (1-\nu_j(t))^\alpha} \frac{d\nu_j(t)}{dt} \quad (5)$$

If all Renyi entropies have the same sign of derivative, local convertibility is present (at least in one direction), and otherwise it is absent. From Eq. (5) we can see that absence of local convertibility is related with not all of the eigenvalues having the same sign of derivative $\frac{d\nu_j}{dt}$, which we will use to interpret the results in the following sections.

III. RESULTS FOR UNFRUSTRATED XY CHAIN

A. Ising chain

Local convertibility in unfrustrated Ising chain was studied in Ref. [16]. Here we will summarize some of

the key ideas and results. As described in the Appendix, Ising (and more generally XY) model is exactly solved through Jordan-Wigner transformation that nonlocally maps the Hamiltonian (1) to a system of free, spinless fermions. This mapping creates a Kitaev chain [19] which can support Majorana fermion edge states. Generally, each Dirac fermion satisfying $\{\psi, \psi\} = 0$ and $\{\psi, \psi^\dagger\} = 1$ can be used to define two Majorana fermions with

$$c_1 = \psi^\dagger + \psi, \quad c_2 = i(\psi - \psi^\dagger), \quad (6)$$

and Majorana fermions satisfy $c_i^\dagger = c_i$, $\{c_i, c_j\} = 2\delta_{ij}$. Thus, each fermionic site is doubled in two Majorana fermionic sites. Edge states form at the boundaries of a system (or subsystem) if parameters of the Hamiltonian are such that the interactions between Majorana fermions belonging to neighboring sites are stronger than the on-site interactions, as illustrated on Fig. 3. In XY chain, on-site interactions correspond to interaction with external magnetic field and inter-site interactions correspond to interactions between the spins, which are dominant for $h < 1$, i. e. in (anti)ferromagnetic phase [16].

Results for sign of derivative of Renyi entropies as field strength h is varied are shown on Fig. 4. In paramagnetic phase, local convertibility is always present, and entanglement decreases as h is increased which is expected since for in the limit of very large h Ising model reduces to almost independent spins in external field. On the other hand, for $h < 1$ and small subsystem size (e. g. $L = 2$), local convertibility is absent in both directions due to edge state recombination. When L is increased, edge state recombination effects become less prominent since subsystem size is much larger than correlation length, except in close vicinity of phase transition. As L is increased more and more, region where local convertibility is absent gets smaller and smaller, and local convertibility is restored through almost all of $h < 1$ phase.

Further insight in relevant physics can be gained by directly looking into correlation matrix eigenvalues ν_j (Fig. 4b). From Eq. (4) we can see that correlation matrix eigenvalues can be interpreted as kind of occupation numbers for excitations of a block that corresponds to the subsystem of interest [16], with $\nu_j = 0$ (boundary eigenvalue) indicating half-filled excitation in ground state and $\nu_j = 1$ (bulk eigenvalue) indicating either completely occupied or completely absent excitation. In $h < 1$ phase, there is an excitation that is neither occupied nor empty, corresponding to unpaired Majorana edge states that were generated by partitioning the chain. As h increases, occupation number of this excitation also increases, most rapidly around the $h = 1$ critical line, which is a direct mark of edge state recombination.

B. Effects of factorization line

Choosing a trajectory that crossed the factorization circle $h^2 + \gamma^2 = 1$ leads to qualitative changes in behavior of local convertibility, although there is no phase

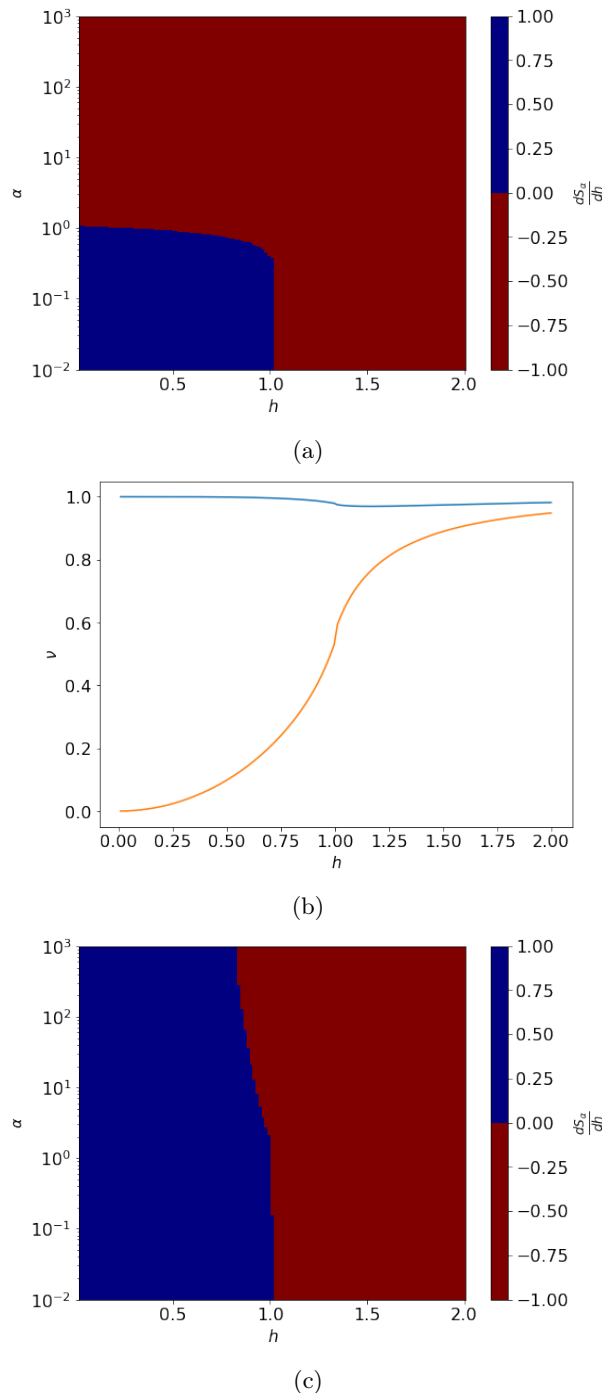


FIG. 4: Ising model with $N = 100$. Sign of $\frac{dS_\alpha}{dh}$ (a) and correlation matrix eigenvalues (b) for $L = 2$; sign of $\frac{dS_\alpha}{dh}$ for $L = 20$ (c).

transition. On the factorization line, ground state is exactly degenerate even for finite N and a factorized state exists in the ground state subspace. In spite of the fact that factorized state does not have definite parity, and in our calculation we follow the ground state with definite parity, for large L there is a minimum of entanglement

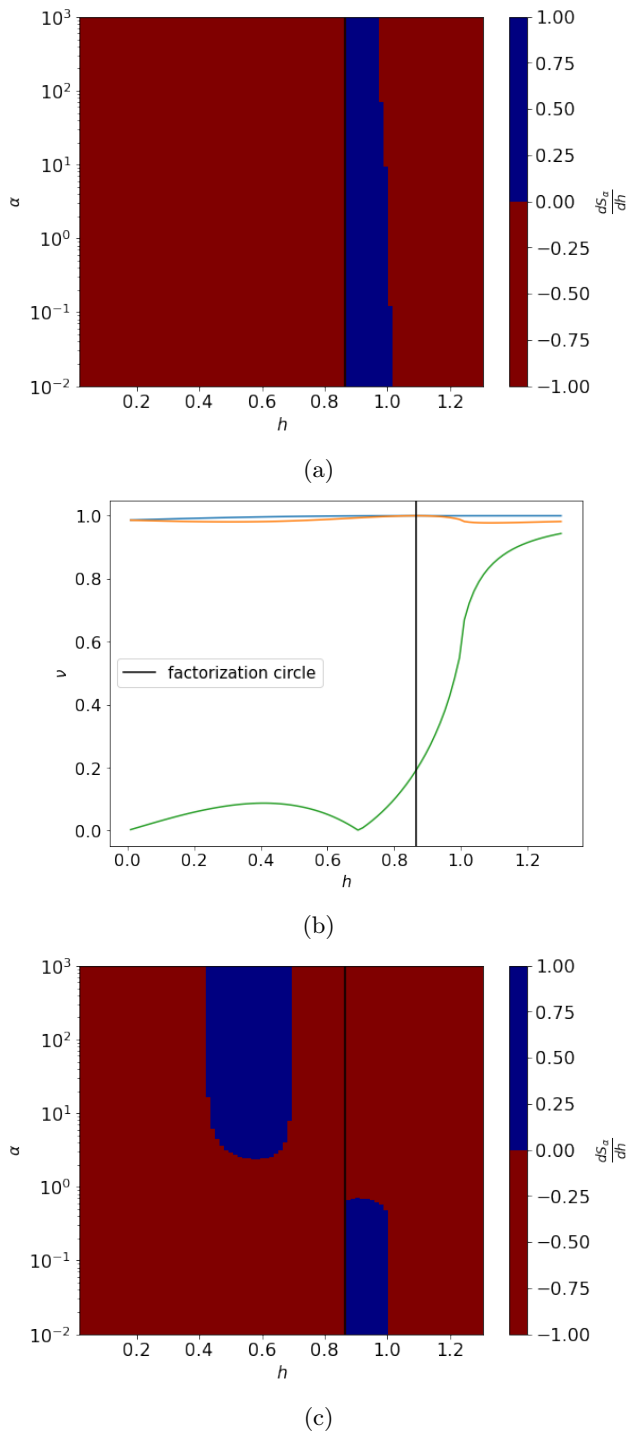


FIG. 5: Unfrustrated XY model, trajectory with constant $\gamma = 0.5$. Sign of $\frac{dS_\alpha}{dh}$ for $L = 50$, $N = 151$ (a), correlation matrix eigenvalues (b) and sign of $\frac{dS_\alpha}{dh}$ (c) for $L = 3$, $N = 101$. Factorization circle is denoted as a black vertical line.

on the factorization line, and signs of $\frac{dS_\alpha}{dt}$ are changed. For any L , Schmidt rank of even ground state on factorization line is 2, so Renyi-0 entropy is equal to $\log 2$ and small α Renyi entropies always have a minimum on the factorization line. The change of signs of $\frac{dS_\alpha}{dt}$ is clearly seen on Fig. 5a in the limit of a large subsystem, where effects of edge state recombination are negligible.

Typical behavior of local convertibility for small L can be seen on Fig. 5c. Because of edge state recombination, local convertibility is absent through the part of (anti)ferromagnetic phase outside of the factorization line. However, in the oscillatory region, there are alternating subregions where local convertibility is present and absent. As noted before, small α Renyi entropies decrease as factorization line is approached, while higher Renyi entropies can both increase and decrease because of oscillations of the boundary eigenvalue (Figure 5b). Local convertibility is restored if all eigenvalues have the same sign of derivative and this is typically the case close to the factorization line.

By choosing different L , N and for different trajectories in parameter space, we can see that qualitatively local convertibility depends only on the region of parameter space we are moving through. Contrary to expectation, even in $N \rightarrow \infty$ limit, local convertibility is not a property of the quantum phase as it can be both present and absent along trajectories in the oscillatory region. It only becomes a property of the phase if both system and subsystem sizes are large, leading to suppression of edge state recombination and oscillations of eigenvalues in the oscillatory region, but even in that case signs of Renyi entropy derivatives are changed on the factorization line.

IV. RESULTS FOR FRUSTRATED XY CHAIN

Presence of frustration modifies the correlation functions and affects local convertibility in qualitatively different ways depending on the region of XY model parameter space. In paramagnetic phase, correlation functions are not modified at all in a frustrated system. In region with $1 - \gamma^2 < h < 1$, energy associated with exciting π momentum mode becomes negative, leading to a modification of correlation functions (Eqs (A11) and (A15)). Finally, in the chiral region ($h < 1 - \gamma^2$), ground state becomes exactly two-fold degenerate, its parity switches between even and odd and it acquires momentum (see Eq. (A16) and the discussion in the Appendix). Corresponding Majorana correlation functions are given by Eqs (A21) and (A22). Since there is a finite number of correction terms to correlation functions that arise from frustration, and these terms are scaled with $1/N$, in thermodynamic limit correlation functions converge to unfrustrated ones. Because of this, for large N there is a change in local convertibility behavior as the factorization line $h^2 + \gamma^2 = 1$ of unfrustrated model is crossed, although the factorization line does not exist for a frustrated XY chain.

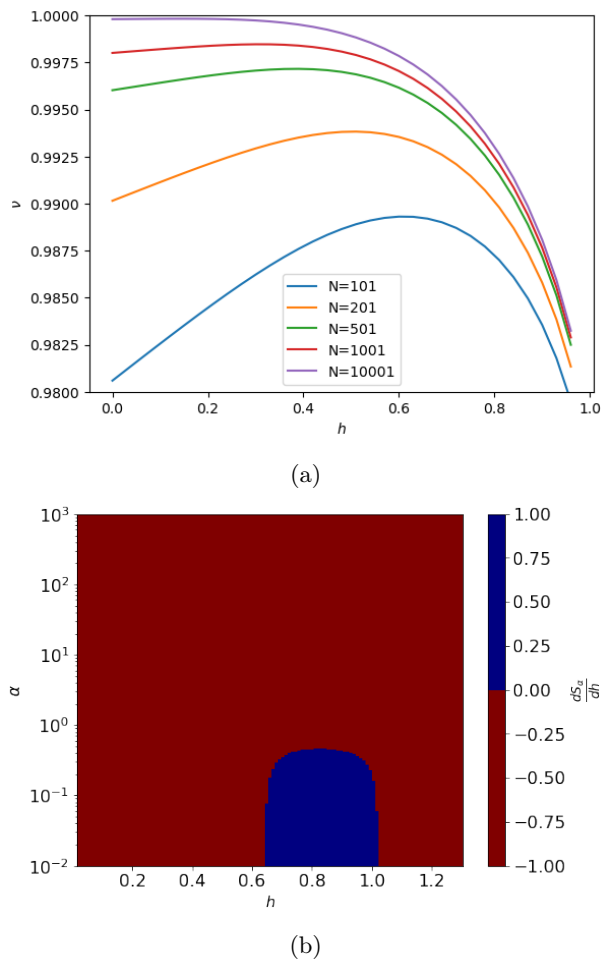


FIG. 6: Approach of bulk correlation matrix eigenvalue to thermodynamic limit (a), and sign of $\frac{d\lambda}{dh}$ for frustrated Ising model with $L = 2$, $N = 101$ (b).

A. Approach of correlation functions to thermodynamic limit

Some properties of approach of correlation functions to thermodynamic limit can be inferred analytically from the scaling of Frobenius norm of correlation matrices. Frobenius norm is defined with $\|M\| = \sqrt{\sum_{ij} |M_{ij}|^2}$. We look into scaling of $\|C - C_{nf}\|$ with system size N . C and C_{nf} denote frustrated and non-frustrated correlation matrices, respectively.

From the Majorana correlation functions derived in the Appendix, we can see that in antiferromagnetic phase there are $O(L^2)$ contributions from frustration to the correlation matrix, and each of these contributions scales as $O(1/N)$. Therefore, if L is fixed, in the thermodynamic limit frustrated correlation matrix will converge to the non-frustrated one. However, as non-frustrated correlation matrix converges to its thermodynamic limit very quickly, Frobenius norm $\|C - C_{nf}\|$ will be dominated by contributions from frustration and it converges to zero

slowly, as $1/N$. Correspondingly, effects of frustration on correlation functions and local convertibility can be non-negligible even for large N . On the other hand, if L is scaled with N so that L/N ratio is kept fixed, number of contributions to the correlation matrix scales with $O(N^2)$, and Frobenius norm converges to a fixed limit, $\lim_{N \rightarrow \infty} \|C - C_{nf}\| = 2\sqrt{2}\frac{L}{N}$.

Unfrustrated systems with large L and N generally have $L - 1$ bulk eigenvalues that are close to 1, and a single boundary eigenvalue that is approximately 0 through the $h < 1$ phase. Frustrated systems have an additional eigenvalue different from 1 that converges to $1 - 2L/N$, which is consistent with the limit of Frobenius norm. Physical interpretation of the eigenvalue approaching $1 - 2L/N$ is that it comes from a single excitation present in a frustrated system that is equally distributed along the chain, which can be seen from its contribution $(1 \pm \nu_j)/2$ to RDM eigenvalues.

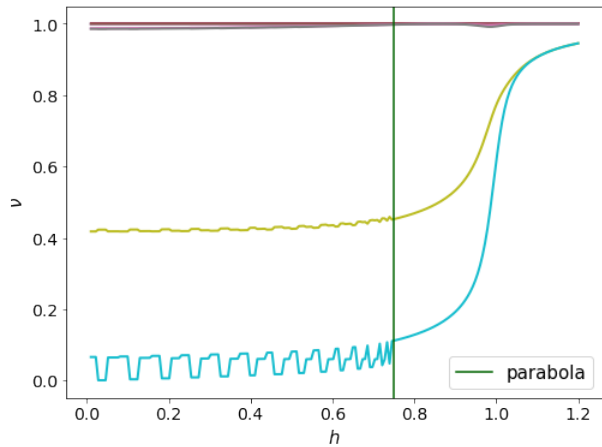
B. $\sqrt{1 - \gamma^2} < h < 1$ region

Between the factorization circle and $h = 1$ critical line, for small L generally there is no local convertibility due to edge state recombination. However, there are exceptions when local convertibility is partially or completely restored for finite N . This happens because in a frustrated model, bulk eigenvalues are not equal to 1 at the $h^2 + \gamma^2 = 1$ circle except in thermodynamic limit. If bulk eigenvalues happen to have the same sign of derivative as the boundary eigenvalue, local convertibility will be restored. An example can be seen on Figure 6 for Ising model whose antiferromagnetic phase is contained in this region. The factorization point corresponds to the classical point $(\gamma, h) = (1, 0)$.

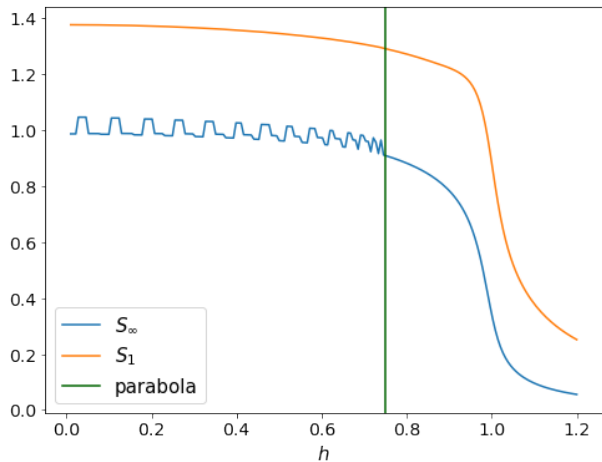
If L/N ratio is kept constant in thermodynamic limit, typically the additional non-bulk eigenvalue has the same sign of derivative as the boundary eigenvalue through $h > \sqrt{1 - \gamma^2}$ region, and the opposite sign from the bulk eigenvalues. This leads to the absence of local convertibility for finite N , as higher α Renyi entropies will decrease towards the $h = 1$ critical line. However, in the $N \rightarrow \infty$ limit local convertibility is restored as the derivatives of all eigenvalues tend to 0.

C. $1 - \gamma^2 < h < \sqrt{1 - \gamma^2}$ region

Local convertibility is at least partially restored for any L and N through the region between the $h = 1 - \gamma^2$ parabola and factorization line (Fig. 7). This is due to the fact that bulk eigenvalues increase towards the factorization line, where they reach a maximum that corresponds to zero entanglement on the factorization line for the unfrustrated system. The mechanism by which local convertibility is restored is the same as in the last subsection: the boundary eigenvalues increase through the



(a)



(b)

FIG. 7: Frustrated XY chain, trajectory with constant $\gamma = 0.5$, $L = 30$, $N = 91$. (a) Correlation matrix eigenvalues, (b) S_1 (von Neumann) and S_∞ Renyi entropies.

antiferromagnetic phase, so their sign of derivative coincides with signs of derivatives of bulk eigenvalues close to the factorization line. It is interesting to note that the frustrated XY chain can "see" the existence of factorization line in unfrustrated chain due to the fact that correlation functions of both chains are the same in thermodynamic limit.

D. $h < 1 - \gamma^2$ region

In the chiral region, we observe that correlation matrix eigenvalues oscillate because of changing ground state momentum. Furthermore, as for finite N allowed momenta are discrete changes, ground state momentum changes discontinuously and correlation matrix eigenvalues also have discontinuities along the path in parameter

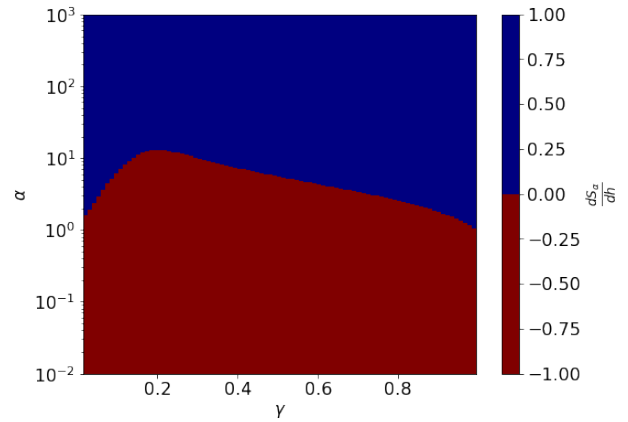


FIG. 8: Sign of $\frac{dS_\alpha}{dh}$ for frustrated XY model with $L = 100$, $N = 201$, trajectory along $h = 0.5(1 - \gamma^2)$ parabola.

space. This implies that the derivatives of correlation matrix eigenvalues and Renyi entropies cannot be defined, we can only study finite Renyi entropy differences between two points in parameter space and infer local convertibility properties from these differences.

Despite this, for fixed L and in $N \rightarrow \infty$ limit, frustration becomes a vanishing contribution, and there are no discontinuities in ground state momenta. The local convertibility behaviour for large N is determined by local correlations that are the same as in unfrustrated model which leads to qualitatively similar results for frustrated and unfrustrated models.

On the other hand, if L/N ratio is kept fixed while N is increased, local convertibility is absent because of oscillations and discontinuities in correlation matrix eigenvalues (Fig. 7). Oscillations are the largest for the boundary eigenvalue, and consequentially for high- α Renyi entropies. For other eigenvalues and for small- α Renyi entropies, unfrustrated contributions from bulk eigenvalues dominate. In $N \rightarrow \infty$ limit, both the amplitude and the period of oscillations decrease as $1/N$. Thus, correlation matrix eigenvalues also become continuous, but nowhere differentiable functions of trajectory parameter t .

To avoid discontinuities in ground state momenta, we can fix both ground state momentum and parity by choosing a trajectory in $\gamma - h$ plane along $h = c(1 - \gamma^2)$ parabola, with $0 \leq c \leq 1$. Generally the bulk eigenvalues increase when we move from $\gamma = 0$ critical line towards the classical point $(\gamma, h) = (1, 0)$ which lies on the factorization line. As the boundary eigenvalues decrease towards the classical point, local convertibility is absent for finite size systems as shown on Fig. 8, but it is recovered in thermodynamic limit as the derivatives of all eigenvalues tend to zero.

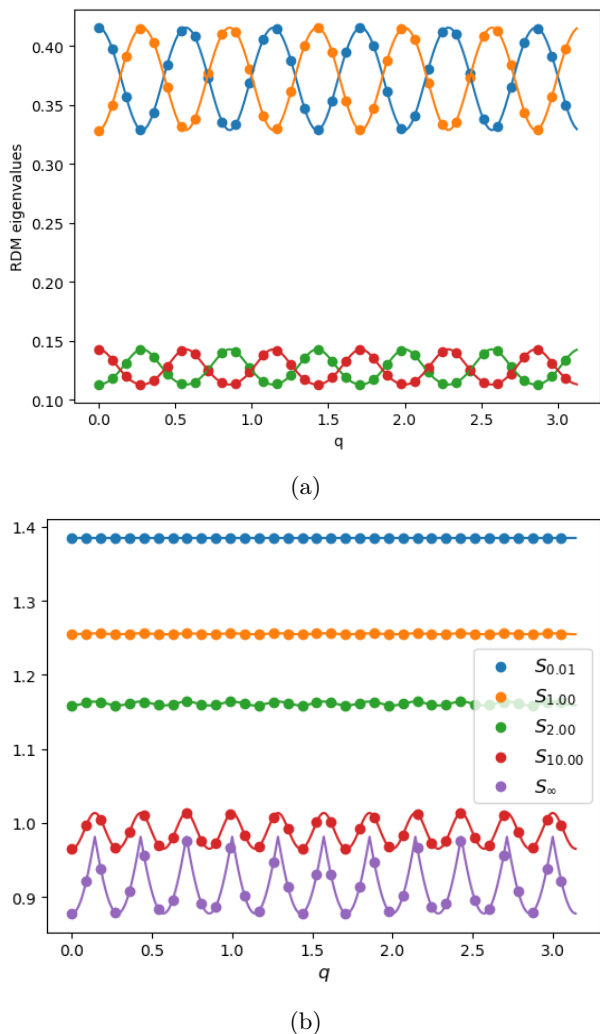


FIG. 9: RDM eigenvalues (a) and Renyi entropies (b) of generalized W states with $N = 35$, $L = 11$. Scattered points are evaluated at allowed momenta, lines show results from Eq. (9) for continuous momenta.

E. Generalized W states

Important insights in local convertibility properties of topologically frustrated models can be gained from local convertibility of W states generalized to finite momentum, defined with

$$|W_q\rangle = \frac{1}{\sqrt{2^N}} \sum_{j=1}^N \exp(iqj) (|j\rangle + |j'\rangle) \quad (7)$$

$|j\rangle = |\dots + - + + - \dots\rangle$ and $|j'\rangle = |\dots - + - - + \dots\rangle$ denote kink states with 2 aligned spins on positions j and $j + 1$, while $|+\rangle$ and $|-\rangle$ are eigenstates of σ^x operator, $\sigma^x |\pm\rangle = \pm |\pm\rangle$. Allowed lattice momenta q for a chain with N spins are $q \in \{\frac{\pi n}{N}\}_{n=0}^{2^N-1}$. Generalized W states have the same entanglement properties as the original W

states [20]

$$|W\rangle = \frac{1}{\sqrt{2^N}} \sum_{j=1}^N \sigma_j^z |-\rangle^{\otimes N}, \quad (8)$$

and can be obtained from them using a Clifford circuit which can be efficiently simulated on a classical computer.

Close to the classical point, ground state of a topologically frustrated spin chain can be approximated with $|W_q\rangle$ state that has the same momentum [21]. Classical point is defined as the point in parameter space where the Hamiltonian reduces to Ising model in zero external field. Thus, we can study the contribution to entanglement and local convertibility that originates from topological frustration by considering the properties of generalized W states.

For subsystem size $L \geq 2$, RDM of W state always has exactly 4 non-zero eigenvalues. The non-zero eigenvalues are given with

$$\lambda_{1,\dots,4} = \frac{1}{4N} \left(N + 2\chi \cos(qL) \pm \sqrt{(N - 2L)^2 + 4N(1 + \chi \cos(qL)) - 4 \sin^2(qL)} \right), \quad (9)$$

where $\chi = \pm 1$. RDM eigenvalues have oscillations with period in momentum equal to $2\pi/L$, as seen from Eq. (9) and on Fig. 9a. This corresponds to $L/2$ full periods between $q = 0$ and $q = \pi$, which is the same as the number of oscillations observed for a frustrated XY chain (Fig. 7) It is also straightforward to show by differentiation that RDM eigenvalues have minima and maxima at $k\pi/L$, $k \in \mathbb{Z}$. In thermodynamic limit, two eigenvalues tend to $L/2N$, and the other two tend to $(N - L)/2N$, independently of momentum q . Amplitude of oscillations scales as $1/N$, except in the case when L is scaled with N so that $N = 2L + \text{const.}$, when the amplitude scales as $1/\sqrt{N}$ (see the Appendix). If L is scaled linearly with N , period of oscillations also scales as $1/N$, so the eigenvalues become constant, but nowhere differentiable functions of momentum.

Due to the oscillations of eigenvalues, there are also oscillations in Renyi entropies. Between any two allowed momenta, all Renyi entropies either increase or decrease (see Fig. 9b and the Appendix), implying presence of local convertibility. However, Renyi entropies oscillate with a period of π/L and have a series of minima and maxima, so the direction of local convertibility changes and local convertibility is not present if q is swept along the whole range of W state momenta. For fixed L , oscillation period is constant, and their amplitude goes to 0 for large N , so local convertibility is restored in thermodynamic limit. However, if L is scaled with N , oscillations in $\alpha = \infty$ Renyi entropy $S_\infty = -\log(\lambda_{max})$ will scale as $1/N$ (or $1/\sqrt{N}$ if $N = 2L + \text{const.}$), and $S_\infty(q)$ will tend to a constant, nowhere differentiable function. Amplitude of oscillations in $\alpha < \infty$ Renyi entropies scales

as $1/N^2$, so the oscillations disappear in thermodynamic limit.

V. CONCLUSION

Our results reveal several features of local convertibility in XY chain and more broadly topologically frustrated systems. Somewhat unexpectedly, we found that local convertibility is not a property of quantum phase except if both system and subsystem size are taken to infinity. This is the case for both frustrated and unfrustrated models. Also, the presence of factorization line in unfrustrated and chiral region in frustrated XY model can have effects on local convertibility and entanglement that are in some aspects reminiscent of a phase transition.

We have shown that features of the unfrustrated model, more specifically the factorization line, can significantly influence the local convertibility of the frustrated model. This is explained by the fact that correlation functions of frustrated model converge to those of unfrustrated model for large system size. We can expect such "cross-talk" of frustrated and unfrustrated XY chain to show up in other topologically frustrated models, too, as there is always a single excitation from frustration whose contribution to correlation functions vanishes in thermodynamic limit.

In the chiral region of frustrated XY chain, due to discontinuities in ground state momentum we can no longer define Renyi entropy derivatives and we observe completely different behavior of local convertibility. Perhaps the most interesting effect is the appearance of fractal-like structure when Renyi entropies are evaluated, since both amplitude and period of oscillations scale as $1/N$ in $N \rightarrow \infty$ limit. These oscillations lead to absence of local convertibility for any finite system size. Also, to observe the effect, we have to simultaneously take $N \rightarrow \infty$ and $L \rightarrow \infty$ limits while keeping $L/N = \text{const.}$, because the effect is completely absent if we take $N \rightarrow \infty$ limit independently of L . In the latter case, corrections to correlation functions due to FBC go to zero, while neglecting the growing number of corrections in the correlation matrix which leads to a finite effect. Physically, this means that there is another relevant length scale in the system, which is the system size N . In unfrustrated models, the only length scale relevant for local convertibility was the correlation length, and increasing correlation length was able to destroy local convertibility through edge state recombination as phase transition is approached. Presence of frustration is introduced by choosing the boundary conditions, so the only scale related to it is the system size. Relevance of system size for local convertibility of frustrated systems is directly confirmed by the fact that we need to consider subsystem size that is scaled with N in order to fully characterize local convertibility and to observe effects such as the aforementioned oscillations of Renyi entropies.

Finally, we have connected the local convertibility

properties of frustrated XY model to a wide class of topologically frustrated models by analyzing local convertibility of generalized W states that form the underlying structure of ground states near the classical point. We showed that Renyi entropies of W states oscillate due to the changing momentum and have the same oscillation period, and for finite size chains they also have discontinuities because of discrete lattice momenta. These oscillations lead to absence of local convertibility along a path in parameter space, even though the states corresponding to the end points of the trajectory are always locally convertible. If subsystem size is scaled with the system size, the oscillations persist in thermodynamic limit in the sense that Renyi entropies are not differentiable functions of momentum. All these results are in direct correspondence with the results for frustrated XY chain and allow us to gain deeper understanding of our numerical results, and to conclude that the effects of frustration on local convertibility we observed in XY chain are a general property of frustrated spin chains.

Appendix A: Frustrated XY chain solution and correlation functions

The solution presented here is based on [11]. Spin operators in Eq.(1) are mapped to (Dirac) fermionic ones through Jordan-Wigner transformation:

$$\sigma_j^- = \prod_{l<j} \sigma_l^z \psi_j^\dagger, \quad \sigma_j^+ = \prod_{l<j} \sigma_l^z \psi_j, \quad \sigma_j^z = 1 - 2\psi_j^\dagger \psi_j \quad (\text{A1})$$

Fermionic operators satisfy standard anticommutation relations

$$\{\psi_i, \psi_j\} = 0, \quad \{\psi_i, \psi_j^\dagger\} = \delta_{ij}, \quad (\text{A2})$$

which can be shown from their definition and Pauli matrix commutation relations.

The Hamiltonian becomes (h.c. stands for hermitian conjugate)

$$H = \sum_{j=1}^{N-1} (\psi_j^\dagger \psi_{j+1} + \gamma \psi_{j+1} \psi_j + h.c.) + 2h \sum_{j=1}^N \psi_j^\dagger \psi_j + \Pi_z (\psi_1^\dagger \psi_N + \gamma \psi_1 \psi_N + h.c.), \quad (\text{A3})$$

which can be decomposed into even and odd parity sectors as

$$H = \frac{1 + \Pi_z}{2} H^+ + \frac{1 - \Pi_z}{2} H^- + \frac{1 - \Pi_z}{2} H^- - \frac{1 - \Pi_z}{2} \quad (\text{A4})$$

where H^\pm are quadratic in fermionic operators. The Hamiltonian can be diagonalized by performing Fourier transform

$$\psi_q = \frac{e^{-i\pi/4}}{\sqrt{N}} \sum_{j=1}^N e^{-iqj} \psi_j \quad (\text{A5})$$

followed by Bogoliubov rotation

$$b_q = \cos \theta_q \psi_q + \sin \theta_q \psi_{-q}^\dagger \quad (\text{A6})$$

Here $q \in \Gamma^- = \{\frac{2\pi n}{N}\}_{n=0}^{N-1}$ in the odd parity sector, or $q \in \Gamma^+ = \{\frac{2\pi(n+1/2)}{N}\}_{n=0}^{N-1}$ in the even parity sector and

$$\theta_q = \frac{1}{2} \arctan\left(\frac{\gamma \sin q}{h + \cos q}\right), \quad q \neq 0, \pi, \quad \theta_{0,\pi} = 0 \quad (\text{A7})$$

With these transformations, we obtain the Hamiltonians in odd and even parity sectors:

$$H^- = \sum_{q \in \Gamma^- - \{0\}} \Lambda(q) (b_q^\dagger b_q - \frac{1}{2}) + \epsilon(0) (b_0^\dagger b_0 - \frac{1}{2}) \quad (\text{A8})$$

$$H^+ = \sum_{q \in \Gamma^+ - \{\pi\}} \Lambda(q) (b_q^\dagger b_q - \frac{1}{2}) + \epsilon(\pi) (b_\pi^\dagger b_\pi - \frac{1}{2}) \quad (\text{A9})$$

Dispersion relation is given with

$$\Lambda(q) = |h + \cos q + i\gamma \sin q|; \quad q \neq 0, \pi \quad (\text{A10})$$

$$\epsilon(0) = h + 1, \quad \epsilon(\pi) = h - 1 \quad (\text{A11})$$

For $h > 1$ and $1 - \gamma^2 \leq h \leq 1$, ground state has even parity and is non-degenerate for a finite number of spins (if $1 - \gamma^2 \leq h \leq 1$ energy gap closes in thermodynamic limit). When $h < 1 - \gamma^2$, ground state is two-fold degenerate even for finite number of spins and its parity switches between even and odd sectors depending on precise values of h , γ and N , with progressively denser crossings for large N .

To calculate correlation functions, we introduce Majorana fermionic operators

$$A_i = \psi_i^\dagger + \psi_i, \quad B_i = i(\psi_i - \psi_i^\dagger) \quad (\text{A12})$$

Using Wick's theorem, all spin correlation functions can be calculated from $\langle A_l A_j \rangle$, $\langle B_l B_j \rangle$ and $\langle A_l B_j \rangle$ (anticommutation relations imply $\langle B_j A_l \rangle = -\langle A_l B_j \rangle$).

In unfrustrated XY chain, the ground state is Bogoliubov vacuum, and it can be shown that

$$\langle A_l A_j \rangle = \langle B_l B_j \rangle = \delta_{lj} \quad (\text{A13})$$

$$\langle B_j A_{j+r} \rangle = \frac{i}{N} \sum_{q \in \Gamma^+} (\sin(2\theta_q) \sin(qr) + \cos(2\theta_q) \cos(qr)) \quad (\text{A14})$$

This expression is valid in the whole parameter space. For $h > 1$, there are no differences between frustrated and unfrustrated correlation functions, and in both cases ground state is the Bogoliubov vacuum state in the even parity sector $|0^+\rangle$ (state that is annihilated by all operators b_q).

For $1 - \gamma^2 \leq h \leq 1$, energy associated with π momentum mode in frustrated chain becomes negative, but ground state is still the Bogoliubov vacuum $|0^+\rangle$ due to parity constraints. We still have $\langle A_l A_j \rangle = \langle B_l B_j \rangle = \delta_{lj}$, but there is an additional contribution to correlation functions $\langle B_j A_{j+r} \rangle$:

$$\begin{aligned} \langle B_j A_{j+r} \rangle &= \frac{2i(-1)^r}{N} + \\ &+ \frac{i}{N} \sum_{q \in \Gamma^+} (\sin(2\theta_q) \sin(qr) + \cos(2\theta_q) \cos(qr)) \end{aligned} \quad (\text{A15})$$

For $h < 1 - \gamma^2$, the dispersion relation has two minima at $q = \pm \tilde{q}$, where

$$\tilde{q} = \arccos\left(\frac{h}{\gamma^2 - 1}\right) \quad (\text{A16})$$

For finite number of sites, \tilde{q} is generally not allowed momentum, so we define \tilde{q}^+ and \tilde{q}^- as allowed momenta closest to \tilde{q} in even and odd sector, respectively. States with lowest energy in odd parity sector are $|\pm \tilde{q}^-\rangle = b_{\pm \tilde{q}^-}^\dagger |0^-\rangle$, with energy

$$E_o = \Lambda(\tilde{q}^-) - \frac{\epsilon(0)}{2} - \frac{1}{2} \sum_{q \in \Gamma^- - \{0\}} \Lambda(q) \quad (\text{A17})$$

while in the even parity sector, states with lowest energy are $|\pm \tilde{q}^+\rangle = b_{\pm \tilde{q}^+}^\dagger b_\pi^\dagger |0^+\rangle$ with energy

$$E_e = \Lambda(\tilde{q}^+) + \frac{\epsilon(\pi)}{2} - \frac{1}{2} \sum_{q \in \Gamma^+ - \{\pi\}} \Lambda(q) \quad (\text{A18})$$

Ground state is exactly two-fold degenerate even for finite system size, and its parity switches between even and odd sectors depending on h , γ and N . However, by moving along the parabola $h = c(1 - \gamma^2)$ with $0 \leq c \leq 1$, ground state momentum and parity can be fixed.

We can write the ground state as

$$|g^-\rangle = (ub_{\tilde{q}^-}^\dagger + vb_{-\tilde{q}^-}^\dagger) |0^-\rangle \quad (\text{A19})$$

if it belongs to the odd parity sector ($|u|^2 + |v|^2 = 1$), or

$$|g^+\rangle = b_\pi^\dagger (ub_{\tilde{q}^+}^\dagger + vb_{-\tilde{q}^+}^\dagger) |0^+\rangle \quad (\text{A20})$$

if it belongs to the even parity sector. The Majorana correlation functions are:

$$\langle A_j A_{j+r} \rangle = \langle B_j B_{j+r} \rangle = \delta_{0,r} + \frac{2i}{N} (|v|^2 - |u|^2) \sin(r\tilde{q}^\pm) \quad (\text{A21})$$

$$\begin{aligned} \langle B_j A_{j+r} \rangle &= \frac{i}{N} \sum_{q \in \Gamma^\pm} (\sin(2\theta_q) \sin(qr) + \cos(2\theta_q) \cos(qr)) - \\ &- \frac{2i}{N} ((\sin(2\theta_{\tilde{q}^\pm}) \sin(\tilde{q}^\pm r) + \cos(2\theta_{\tilde{q}^\pm}) \cos(\tilde{q}^\pm r)) + \\ &+ \frac{4i}{N} |uv^*| \cos(\tilde{q}^\pm(r+2j) + \alpha) \end{aligned} \quad (\text{A22})$$

where $\alpha = \arg(uv^*)$, + sign is used if ground state is in even sector, and - sign is used if ground state is in odd sector.

Appendix B: Analytical results for generalized W states

All analytical results for generalized W states can be derived starting from the definition of Renyi entropies

$$S_\alpha = \frac{1}{1-\alpha} \log(\lambda_1^\alpha + \lambda_2^\alpha + \lambda_3^\alpha + \lambda_4^\alpha) \quad (\text{B1})$$

and the expression for RDM eigenvalues (Eq.(9)). By differentiating Eq. (9) w.r.t. q , we obtain that all eigenvalues have extrema for $q = k\pi/L$, $k \in \mathbb{Z}$. λ_1 and λ_4 have maxima at $q = 2k\pi/L$ and minima at $q = (2k+1)\pi/L$, while λ_2 and λ_3 have minima at $q = 2k\pi/L$ and maxima at $q = (2k+1)\pi/L$.

Scalings of oscillation amplitude can be determined by expanding Eq. (9) in Taylor series for large N . If $N = cL + d$, where $c \in [0, 1/2]$ is kept constant as N is increased, we obtain

$$\lambda_{1,\dots,4} = \frac{1}{4} + \frac{\chi}{2N} \cos(qL) \pm \frac{x}{4} \left(1 + \frac{2}{x^2 N} (1 + \chi \cos(qL)) \right) + O(N^{-2}), \quad (\text{B2})$$

where $x = \lim_{N \rightarrow \infty} (N - 2L)/N$, $x \in \langle 0, 1 \rangle$. If $c = 0.5$, i.e. $x = 0$, we get

$$\lambda_{1,\dots,4} = \frac{1}{4} \pm \frac{1}{2\sqrt{N}} \sqrt{1 + \chi \cos(qL)} + O(N^{-1}) \quad (\text{B3})$$

Renyi entropies have oscillation period of π/L , because translation in momentum $q \rightarrow q + \pi/L$ corresponds to interchanging $\lambda_1 \leftrightarrow \lambda_2$ and $\lambda_3 \leftrightarrow \lambda_4$, so Renyi entropies remain the same. Therefore, we can map a point with arbitrary momentum to $[0, \pi/L]$ interval and study the behaviour of Renyi entropies on this interval. Furthermore, we can map $q \mapsto q$, $q \in [0, \pi/2L]$,

and $q \mapsto \pi/L - q$, $q \in \langle \pi/2L, \pi/L \rangle$. This corresponds to another interchange $\lambda_1 \leftrightarrow \lambda_2$ and $\lambda_3 \leftrightarrow \lambda_4$, so we can confine ourselves to the interval $q \in [0, \pi/2L]$. Derivatives of Renyi entropies are given with

$$\frac{dS_\alpha}{dq} = \frac{\alpha}{1-\alpha} \frac{1}{\lambda_1^\alpha + \lambda_2^\alpha + \lambda_3^\alpha + \lambda_4^\alpha} \times (\lambda_1^{\alpha-1} \frac{d\lambda_1}{dq} + \lambda_2^{\alpha-1} \frac{d\lambda_2}{dq} + \lambda_3^{\alpha-1} \frac{d\lambda_3}{dq} + \lambda_4^{\alpha-1} \frac{d\lambda_4}{dq}) \quad (\text{B4})$$

For general α this expression is not easily simplified, but we ascertained numerically that regardless of α , N and L , all Renyi entropies have minima at $k\pi/L$ and maxima at $(k+1/2)\pi/L$, and that they are increasing functions of q for $q \in [0, \pi/2L]$. To compare Renyi entropies of two generalized W states and determine the direction of local convertibility, we map their momenta to $[0, \pi/2L]$ interval and just determine which momentum is closer to 0. It should be noted that although allowed lattice momenta are not continuous, eigenvalues are well-defined and continuous functions of q generalized to continuous, real numbers and Renyi entropies can be compared using continuous q because Renyi entropies are monotonous on $[0, \pi/2L]$.

Scaling of amplitude of S_∞ Renyi entropy oscillations is obtained by expanding $S_\infty = -\log(\lambda_{max})$ in Taylor series for large N . For $q \in [0, \pi/2L]$, $\lambda_{max} = \lambda_1$. The result is

$$\Delta S_\infty = S_\infty(\pi/2L) - S_\infty(0) = \frac{2}{xN} + O(N^{-2}) \quad (\text{B5})$$

for $x \neq 0$, and

$$\Delta S_\infty = S_\infty(\pi/2L) - S_\infty(0) = (2\sqrt{2} - 2) \sqrt{\frac{1}{N}} + O(N^{-1}) \quad (\text{B6})$$

for $x = 0$.

-
- [1] X. G. Wen, Topological orders in rigid states, International Journal of Modern Physics B **04**, 239 (1990), <https://doi.org/10.1142/S0217979290000139>.
- [2] M. Greiner, O. Mandel, T. Esslinger, T. W. Hänsch, and I. Bloch, Quantum phase transition from a superfluid to a mott insulator in a gas of ultracold atoms, Nature **415**, 39 (2002).
- [3] T. Senthil, S. Sachdev, and M. Vojta, Fractionalized fermi liquids, Phys. Rev. Lett. **90**, 216403 (2003).
- [4] I. Bloch, J. Dalibard, and W. Zwerger, Many-body physics with ultracold gases, Rev. Mod. Phys. **80**, 885 (2008).
- [5] M. A. Nielsen and I. L. Chuang, *Quantum Computation and Quantum Information: 10th Anniversary Edition* (Cambridge University Press, 2010).
- [6] D. Gross, S. T. Flammia, and J. Eisert, Most quantum states are too entangled to be useful as computational resources, Phys. Rev. Lett. **102**, 190501 (2009).
- [7] M. Van den Nest, Universal quantum computation with little entanglement, Phys. Rev. Lett. **110**, 060504 (2013).
- [8] M. A. Nielsen, Conditions for a class of entanglement transformations, Phys. Rev. Lett. **83**, 436 (1999).
- [9] J. Simon, W. S. Bakr, R. Ma, M. E. Tai, P. M. Preiss, and M. Greiner, Quantum simulation of antiferromagnetic spin chains in an optical lattice, Nature **472**, 307 (2011).
- [10] V. Marić, S. M. Giampaolo, and F. Franchini, Quantum phase transition induced by topological frustration, Communications Physics **3**, 220 (2020).
- [11] A. G. Catalano, D. Brtan, F. Franchini, and S. M. Giampaolo, Simulating continuous symmetry models with discrete ones, Phys. Rev. B **106**, 125145 (2022).
- [12] E. Barouch and B. M. McCoy, Statistical mechanics of the xy model. ii. spin-correlation functions, Phys. Rev. A **3**, 786 (1971).
- [13] E. Lieb, T. Schultz, and D. Mattis, Two soluble models

- of an antiferromagnetic chain, *Annals of Physics* **16**, 407 (1961).
- [14] S. Turgut, Catalytic transformations for bipartite pure states, *Journal of Physics A: Mathematical and Theoretical* **40**, 12185 (2007).
- [15] M. Klimesh, Inequalities that collectively completely characterize the catalytic majorization relation (2007), arXiv:0709.3680 [quant-ph].
- [16] L. Amico, V. Korepin, A. Hamma, S. M. Giampaolo, and F. Franchini, Local convertibility in quantum spin systems, in *Entanglement in Spin Chains: From Theory to Quantum Technology Applications*, edited by A. Bayat, S. Bose, and H. Johannesson (Springer International Publishing, Cham, 2022) pp. 151–188.
- [17] M. Z. Hasan and C. L. Kane, Colloquium: Topological insulators, *Rev. Mod. Phys.* **82**, 3045 (2010).
- [18] G. Vidal, J. I. Latorre, E. Rico, and A. Kitaev, Entanglement in quantum critical phenomena, *Phys. Rev. Lett.* **90**, 227902 (2003).
- [19] A. Y. Kitaev, Unpaired majorana fermions in quantum wires, *Physics-Uspekhi* **44**, 131 (2001).
- [20] W. Dür, G. Vidal, and J. I. Cirac, Three qubits can be entangled in two inequivalent ways, *Phys. Rev. A* **62**, 062314 (2000).
- [21] V. Marić, S. M. Giampaolo, D. Kuić, and F. Franchini, The frustration of being odd: how boundary conditions can destroy local order, *New Journal of Physics* **22**, 083024 (2020).